Journal of Statistical Physics, Vol. 54, Nos. 5/6, 1989

Lévy Walks for Turbulence: A Numerical Study

G. Zumofen,[1] A. Blumen,[2] J. Klafter,[3] and M. F. Shlesinger[4]

Received November 9, 1988

We present a numerical study of enhanced diffusion, for which the mean-squared displacement follows asymptotically $\langle r^2(t)\rangle \sim t^\gamma$, $\gamma > 1$. We simulate continuous time random walks with waiting-time distributions which couple the spatial and temporal parameters; this gives rise to Lévy-walks. Our results confirm the theoretically predicted long-time behavior and demonstrate its temporal regime of validity. Furthermore, the simulations document the appearance of (parameter-dependent) transitions between regular and enhanced diffusion regimes.

KEY WORDS: Random walks; Lévy flights; Kolmogorov spectrum; turbulence.

1. INTRODUCTION

Large classes of dynamical processes in disordered media display deviations from simple Brownian motion, a fact manifested through the dependence of the mean-squared displacement $\langle r^2(t)\rangle$ on time. Whereas for simple diffusion $\langle r^2(t)\rangle \sim t$, anomalous diffusion is characterized by

$$\langle r^2(t)\rangle \sim t^\gamma \tag{1}$$

with $\gamma \neq 1$. Examples for Eq. (1) are to be found in chaotic dynamics, which generally leads to enhanced diffusion (e.g., for turbulent motion $\gamma \simeq 3$) on the one hand,[1-9] but also in systems with geometrical constraints (doped crystals, glasses, fractals), for which the diffusion is dispersive, i.e., $\gamma < 1$, on the other hand.[10-14]

[1] Physical Chemistry Laboratory, ETH-Center, CH-8092 Zurich, Switzerland.
[2] Physical Institute and BIMF, University of Bayreuth, D-8580 Bayreuth, FRG.
[3] School of Chemistry, Tel-Aviv University, 69978 Tel-Aviv, Israel.
[4] Physics Division, Office of Naval Research, Arlington, Virginia 22217, USA.

0022-4715/89/0300-1519$06.00/0

In a recent work[15] we have developed an analytical approach based on asymptotic expansions. We have stressed that both patterns of anomalous diffusion follow from a unified stochastic approach, whose basis are continous-time random walks (CTRW).[10,13,16–18] The main ingredients of our approach are spatio-temporal couplings,[19,20] which give rise to Lévy walks.[20–23] In this short communication we focus on a numerical study of Lévy walks. Simulating such processes is extremely valuable, both as a means of visualizing the transport process and also as a possibility to explore crossover regimes, since, in principle, the whole temporal range can be monitored. As a by-product we are able to verify our previous results and to show crossovers at the boundaries between regions of different temporal character.

In the next section we summarize the algebraic approach. In Sec. 3 we present the simulation calculations, and end the paper in Sec. 4 with a discussion of results.

2. THE ANALYTIC APPROACH: CTRW WITH COUPLED MEMORIES

An efficient way to treat the dynamics of stochastic processes consists in following the trajectories of discrete particles: For a discrete underlying space this leads to random walks.[24]

Let $\psi(r, t)$ be the probability distribution of making a step of length r in the time interval t to $t+dt$. The total transition probability in this time interval is

$$\psi(t) = \sum_r \psi(r, t) = \psi(k=0, t) \tag{2}$$

(where, in the last expression we switched to the Fourier space, $r \to k$). Furthermore the survival probability at the initial site is

$$\Phi(t) = 1 - \int_0^t \psi(\tau)\, d\tau \tag{3}$$

so that, reverting to the Laplace space ($t \to u$):

$$\Phi(u) = [1 - \psi(u)]/u \tag{4}$$

In standard fashion[16,25] one has now for the probability density $\eta(r, t)$ of just arriving at r in the time interval t to $t+dt$:

$$\eta(r, t) = \sum_{r'} \int_0^t \eta(r', \tau)\, \psi(r-r', t-\tau)\, d\tau + \delta(t)\, \delta_{r,0} \tag{5}$$

in which the initial condition of starting at $t=0$ from $r=0$ is incorporated. Equation (5) leads to an integral equation for the probability $\rho(r, t)$ that the particle is at r at time t, by observing that

$$\rho(r, t)=\int_0^t \eta(r, t-\tau')\, \Phi(\tau')\, d\tau' \tag{6}$$

With Eq. (6) and a change in the order of the integrations, Eq. (5) is recast into

$$\rho(r, t)=\sum_{r'} \int_0^t \rho(r', \tau)\, \psi(r-r', t-\tau)\, d\tau + \Phi(t)\, \delta_{r,0} \tag{7}$$

Now, turning to the Fourier–Laplace space we have:

$$\rho(k, u)=\rho(k, u)\, \psi(k, u)+\Phi(u) \tag{8}$$

with the solution

$$\rho(k, u)=\frac{1-\psi(u)}{u} \frac{1}{1-\psi(k, u)} \tag{9}$$

One may note that the mean square displacement $\langle r^2(t)\rangle$ is related to $\rho(k, t)$ through:

$$\langle r^2(t)\rangle=\sum_r r^2 \rho(r, t)=-\frac{\partial^2}{\partial k^2} \rho(k, t)\Big|_{k=0} \tag{10}$$

Thus one obtains that in the CTRW formalism the knowledge of $\psi(r, t)$—or, equivalently, of $\psi(k, u)$—determines, via Eqs. (9) and (10), the form of $\langle r^2(t)\rangle$.

Now, as pointed out on several occasions,[9,15,19,20,23] a decoupled spatiotemporal scheme, for which one has

$$\psi(r, t)=\lambda(r)\, \psi(t) \tag{11}$$

is unable to give rise to values γ larger than unity in Eq. (1). On the other hand, such values are typical for turbulent motion, where $\gamma \simeq 3$ holds.[1–9] In order to obtain for $\langle r^2(t)\rangle$ a t^γ behavior with $\gamma>1$ it is imperative to use *coupled* $\psi(r, t)$ forms.[9,15,19,20] A suitable function is[22]

$$\psi(r, t)=C r^{-\mu} \delta(r-t^\nu) \tag{12}$$

which defines the Lévy walks.[9,22] Here, through the δ function, r and t are coupled. Equation (12) allows steps of *arbitrary* length as for

Lévy flights,[28] but long steps are penalized by requiring more time to be performed. Or, stated differently, in a given time window only a finite shell of points may be reached: Hierarchically, nearer points are no more and farther points not yet accessible.

In Ref. 15 we have studied analytically the behavior of $\langle r^2(t)\rangle$ on lattices of arbitrary dimensions d, by using CTRWs where the probability distribution $\psi(r, t)$ is given by Eq. (12). Setting

$$\mu^* = \mu - d + 1 \tag{13}$$

the results for turbulent diffusion ($\gamma > 1$, $\nu > 1/2$) may be summarized as follows (Table I of Ref. 15); for long times one has:

$$\langle r^2(t)\rangle \sim t^{2\nu} \qquad (1 < \nu\mu^* < 2) \tag{14a}$$

$$\langle r^2(t)\rangle \sim t^{2-\nu\mu^*+2\nu} \qquad (2 < \nu\mu^* < 1 + 2\nu) \tag{14b}$$

$$\langle r^2(t)\rangle \sim t \qquad (1 + 2\nu < \nu\mu^*) \tag{14c}$$

Similar relations hold also for dispersive transport ($\gamma < 1$, $\nu < 1/2$).[15] From Eqs. (14) we expect thus in the case $\gamma = 3$, $\nu = 3/2$ crossover effects for $\mu^* = 4/3$ and for $\mu^* = 8/3$. Thus the particular distribution used, Eq. (12), shows a very rich pattern. In the enhanced diffusion regime the turbulent dynamics appears as a special case: The transitions show an intermediate zone between Brownian motion and fully developed enhanced diffusion. We note that this finding is comparable to the transition from Brownian to enhanced motion in ultrametric spaces.[8,14] In the next section we compare Eqs. (14) to numerical simulation results.

3. NUMERICAL SIMULATIONS

In order to clearly visualize the Lévy process involved in Eq. (12) and in order to be able to monitor the full time dependence of $\langle r^2(t)\rangle$ (and not only its asymptotic behavior) we found it expedient to perform numerical simulations.

The procedure is as follows: First, we note from Eq. (13) that the role of the dimension consists in only changing μ to μ^*, and leaving otherwise everything intact. We have thus—for simplicity—centered on the special case $d = 1$, where $\mu = \mu^*$, and have restricted calculations in higher dimensions to consistency checks. Second, from Eq. (12) one has to determine for each step the distance and the time needed to reach the next location. The spatial distribution of location distances follows by integrating over all times

$$\psi(r) = \int_0^\infty dt\, \psi(r, t) = \tilde{C} r^{-\beta} \tag{15}$$

where $\beta = \mu + 1 - \nu^{-1}$. We can now choose a walking distance r according to the distribution (15); the time needed to travel this distance is given, according to Eq. (12), by $t = |r|^{1/\nu}$, Note that for $\nu = 1$ the situation is somewhat similar to random walks in which the walker steps preferentially in the same direction, the so-called persistent (or correlated) random walks.[24-27]

To visualize a realization of such a Lévy walk we present in Fig. 1 the situation for a two-dimensional geometry where we chose $\mu = 3.5$ and $\nu = 1$. For the Lévy walk depicted, a $\langle r^2(t) \rangle \sim t^{3/2}$ behavior is expected, i.e., a behavior intermediate between the t and the t^2 extremal regimes. One

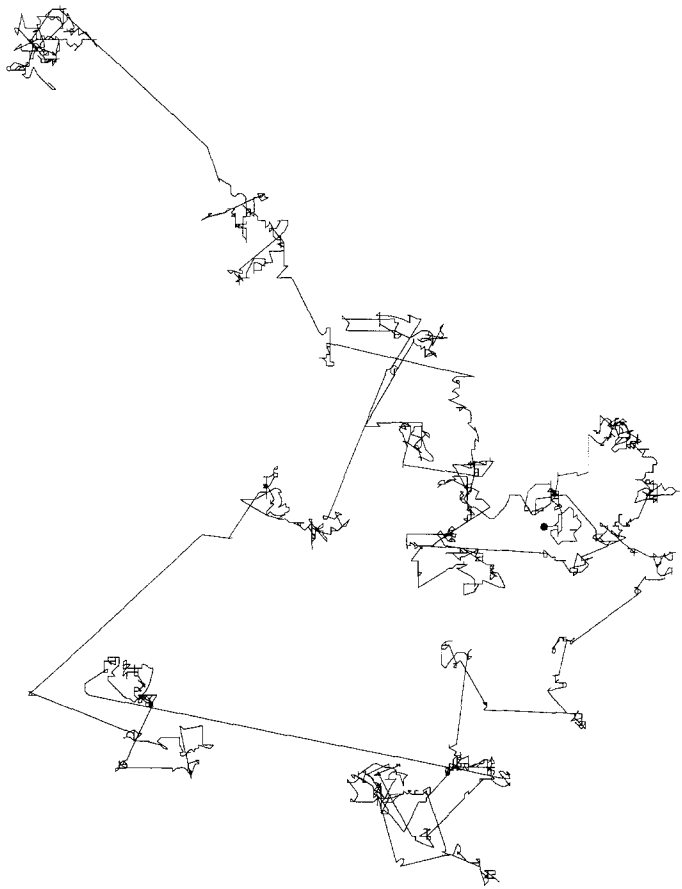

Fig. 1. Realization of a Lévy walk, obtained from the distribution probability, Eq. (12), where $\mu = 3.5$ and $\nu = 1$. The situation depicted evolved after 1000 time units. The starting point of the walk is marked by a dot.

should remark on the self-similar aspect of the picture: a series of small steps is followed by larger ones, which are, after a while, followed by larger ones still; furthermore, no particular length scale dominates. Figure 1 may be compared to the very similar Figs. 296 and 297 of Ref. 28.

To analyze the mean squared displacement for the turbulent case, for which typically $\nu = 3/2$, we display in Fig. 2, $\langle r^2(t) \rangle$ as a function of time. We have varied μ^* between 1 and 3.6 and covered some 4 orders of magnitude in time. For each numerical result (dot) displayed, some 10^4 realizations were used in its averaging. Note the log–log scales; in these scales Eq. (1) corresponds to a straight line of slope γ.

Interestingly, the numerical results do not lie, as a rule, on straight lines; deviations are evident, especially at early times. We have indicated these deviations as dashed curves and used only the numerical results in the late time domain for a least-squares (linear regression) fit. A similar behavior is also obtained for $\nu = 1$, and we present our simulation results together with their analysis in Fig. 3.

For both cases ($\nu = 3/2$ and $\nu = 1$) we summarize in Fig. 4 the slopes γ

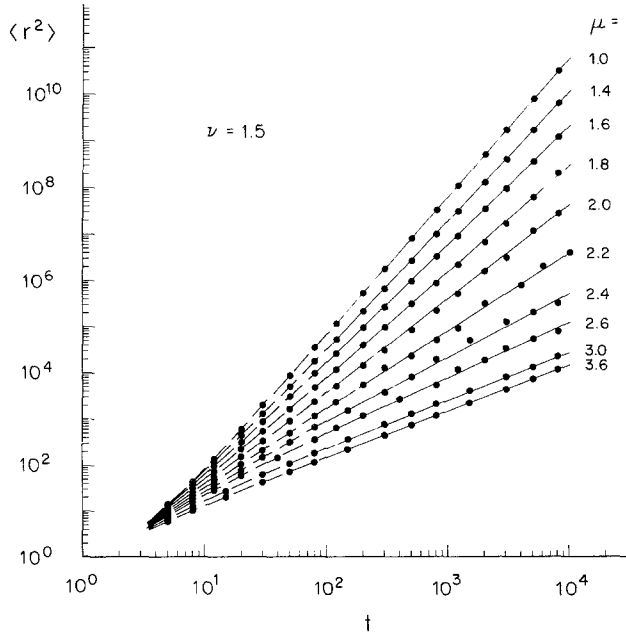

Fig. 2. The mean squared displacement $\langle r^2(t) \rangle$ is indicated as a function of time on log–log scales. Here $\nu = 3/2$ in Eq. (12) and μ is given parametrically. The dots are the result of simulation calculations, the full lines denote the least-squares linear fit, and the dashed lines are guides to the eye.

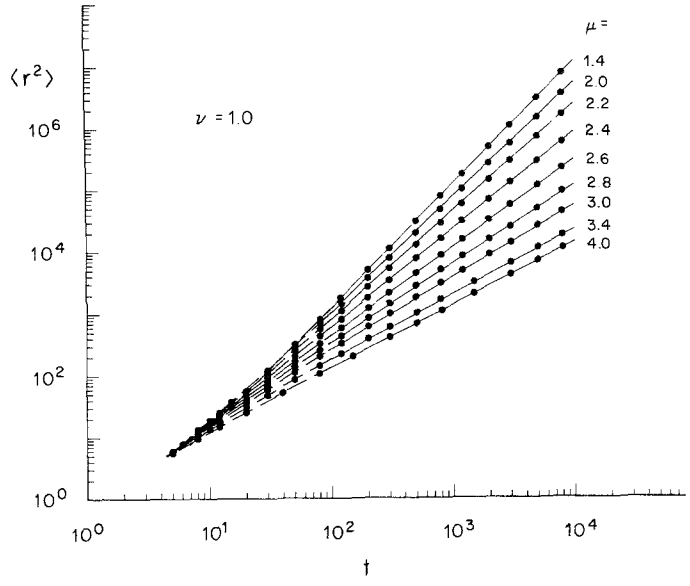

Fig. 3. As in Fig. 2 but for $\nu = 1$.

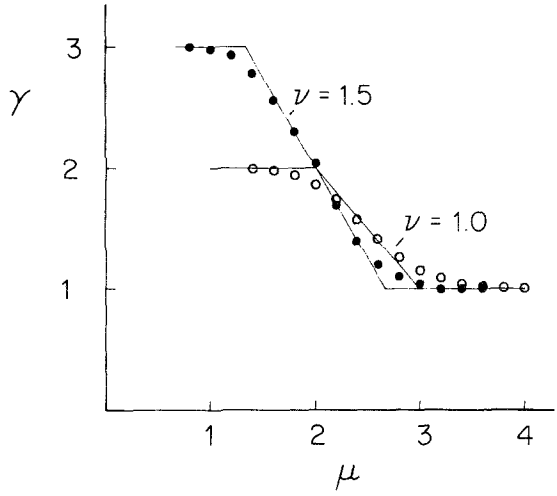

Fig. 4. Summary of the numerically determined asymptotic behavior from Figs. 2 and 3. The slopes are presented as a function of μ; we use dots for $\nu = 3/2$ and circles for $\nu = 1$. The full lines give the analytically expected behavior, Eqs. (14).

obtained by the least-squares-fit. The overall behavior supports very nicely the analytical expressions of Sec. 2. Indeed, the transition regimes $4/3 < \mu^* < 8/3$ for $\nu = 3/2$ and $2 < \mu^* < 3$ for $\nu = 1$ are clearly visible. Furthermore, in both cases the regimes of enhanced diffusion ($\gamma = 3$ or $\gamma = 2$, respectively) and of regular diffusion ($\gamma = 1$) are reached within the time of the numerical experiment. In Fig. 4 we have also indicated through full-lines the theoretically predicted behavior. Whereas the general agreement is good, we also remark that the numerical crossover behavior is considerably *smoother* than theoretically expected: We attribute this to the very long times which are required to reach the asymptotic regime of $\langle r^2(t) \rangle$ for marginal values of μ^* ($\mu^* = 4/3$ and $\mu^* = 8/3$ or $\mu^* = 2$ and $\mu^* = 3$, respectively).

4. CONCLUSIONS

The main conclusion of our present study is that one can use with confidence Lévy walk models in order to model anomalous diffusion in the enhanced ($\gamma > 1$) domain. Whereas deviations from the asymptotic regime are visible at short times, at longer times (factors of 10^3) one has indeed the qualitatively correct behavior; thus the theory works well at time intervals which are of experimental relevance.

A word of caution has to be said for the intermediate regime: as was to be expected, the convergence to the theoretically predicted slopes is particularly slow for the marginal γ values; care has to be exerted there, by monitoring the temporal development over large time scales.

To acquire a fuller picture for the kinematics of turbulence one should compare the computer-simulated motion to experimental findings. Nowadays, careful measurements should become available. Up to now the standard means of marking the velocity regions were by injection of color plumes or by smoke (aerosols, oil fog). These means are not very satisfactory, since one has to put the markers exactly where the vorticity is generated, which taken strictly is impossible;[29] hence on a small scale the interface is marked only roughly. For more precision one has to revert to tracking the molecules of the turbulent flow by themselves. An early proposal was put forth by de Gennes, who suggested using NMR and thermal experiments.[30] We, on the other hand, feel that the method of choice is to use fluorescent probes, which are excited by a laser, so that one attains a high spatial resolution and one does not, through the marking, interfere with the flow process. A series of pictures of jet flows was indeed made visible through luminescence by Dimotakis et al.;[32] it should be expected that this method also allows one to check the validity of the relations developed in this paper.

In summary, tracking enhanced diffusion in turbulent motion could proceed along lines used in the study of dispersive motion in disordered materials, and the Lévy walk–CTRW approach provides a unified theoretical scheme for both types of anomalous diffusion.

ACKNOWLEDGMENTS

A grant of computer time from the Rechenzentrum der ETH-Zürich and the support of the Deutsche Forschungsgemeinschaft (SFB 213) and of the Fonds der Chemischen Industrie are gratefully acknowledged.

REFERENCES

1. A. S. Monin and A. M. Yaglom, *Statistical Fluid Mechanics* (MIT, Cambridge, 1971), Vol. I; (1975), Vol. II.
2. L. F. Richardson, *Proc. R. Soc. London Ser. A* **110**:709 (1926).
3. G. K. Batchelor, *Proc. Cambridge Philos. Soc.* **48**:345 (1952).
4. G. K. Batchelor and A. A. Townsend, in *Surveys in Mechanics*, G. K. Batchelor and A. A. Townsend, in *Surveys in Mechanics*, G. K. Batchelor and R. M. Davies, eds. (Cambridge University Press, 1956), p. 352.
5. A. Okubo, *J. Oceanol. Soc. Jpn.* **20**:286 (1962).
6. H. G. E. Hentschel and I. Procaccia, *Phys. Rev. A* **29**:1461 (1984).
7. S. Grossmann and I. Procaccia, *Phys. Rev. A* **29**:1358 (1984).
8. S. Grossmann, F. Wegner, and K. H. Hoffman, *J. Phys. (Paris) Lett.* **46**:L575 (1985).
9. M. F. Shlesinger and J. Klafter, *Phys. Rev. Lett.* **54**:2551 (1985).
10. H. Scher and E. W. Montroll, *Phys. Rev. B* **12**:2455 (1975).
11. M. F. Shlesinger, *J. Stat. Phys.* **10**:421 (1974).
12. S. Alexander and R. Orbach, *J. Phys. (Paris) Lett.* **43**:L625 (1982).
13. A. Blumen, J. Klafter, B. S. White, and G. Zumofen, *Phys. Rev. Lett.* **53**:1301 (1984).
14. A. Blumen, J. Klafter, and G. Zumofen, in *Optical Spectroscopy of Glasses*, I. Zschokke, ed. (Reidel, Dordrecht, Holland, 1986), p. 199.
15. J. Klafter, A. Blumen, and M. F. Shlesinger, *Phys. Rev. A* **35**:3081 (1987).
16. E. W. Montroll and G. H. Weiss, *J. Math. Phys.* **6**:167 (1965).
17. A. Blumen and G. Zumofen, *J. Chem. Phys.* **77**:5127 (1982).
18. A. Blumen, J. Klafter, and G. Zumofen, in *Fractals in Physics*, L. Pietronero and E. Tossatti, eds. (North Holland, Amsterdam, 1986), p. 399.
19. J. Klafter and R. Silbey, *Phys. Rev. Lett.* **44**:55 (1980).
20. M. F. Shlesinger, J. Klafter, and Y. M. Wong, *J. Stat. Phys.* **27**:499 (1982).
21. H. Takayasu, *Progr. Theor. Phys.* **72**:471 (1984).
22. M. F. Shlesinger and J. Klafter, in *On Growth and Form*, H. E. Stanley and N. Ostrowski, eds. (Nijhoff, Amsterdam, 1985), p. 279.
23. M. F. Shlesinger, B. J. West, and J. Klafter, *Phys. Rev. Lett.* **58**:1100 (1987).
24. G. H. Weiss and R. J. Rubin, *Adv. Chem. Phys.* **52**:363 (1983).
25. J. W. Haus and K. W. Kehr, *Phys. Rep.* **150**:263 (1987).
26. P. Argyrakis and R. Kopelman, *Phys. Rev. B* **22**:1830 (1980).
27. K. Kehr and P. Argyrakis, *J. Chem. Phys.* **84**:5816 (1986).

28. B. B. Mandelbrot, *The Fractal Geometry of Nature* (W. H. Freeman, San Francisco, 1982).
29. K. R. Sreenivasan and C. Meneveau, *J. Fluid Mech.* **173**:357 (1986).
30. P. G. de Gennes, *J. Physique Lett.* **38**:L1 (1977).
31. A. Blumen, G. Zumofen, and J. Klafter, *J. Lumin.* **40/41**:641 (1988).
32. P. Dimotakis, R. C. Lye, and D. Z. Papantoniou, *15th Intl. Symp. Fluid Dyn.*, (Jachranka, Poland, 1981), and Ref. 29.